

# Sea-state Interaction based Lagrangian Dynamic Model of the Liquid Robotics Wave Glider Platform

Gevashkar Rampersadh, Maximillian Finbow, Robyn Verrinder<sup>1</sup> and Edward Boje<sup>1</sup>

**Abstract**—The Liquid Robotics Wave Glider is an unmanned marine research vessels that makes use of wave propulsion to minimise energy requirements during voyages. Models of these hybrid sea-surface and underwater craft must incorporate the platform’s interaction with the sea state to allow for more accurate navigation and path planning. This paper describes the multi-body Wave Glider system using Denavit-Hartenberg parametrisation, with a Lagrangian approach used to generate the equations of motion for the body. Physical dimensions and hydrodynamic factors were derived from both platform measurements and a SolidWorks model of the system. The model’s propulsion is dependent on the sea state by virtue of the characterisation of the hydrofoil motion and the hydrodynamic forces on the hydrofoil. The model is simulated for various sea states to investigate the performance.

## I. INTRODUCTION

Monitoring of marine environments is vital to both marine researchers and industry. Oceanographic variables, such as ocean temperature, chemical analysis, sea state, significant wave height, phytoplankton activity, etc., are conventionally measured by fixed sensor buoys, targeted transects using research vessels, remote satellite imaging or altimetry. Unmanned surface vehicles (USV) and unmanned underwater vehicles (UUV) are being rapidly adopted as a relatively low cost alternative that can complement these approaches. They have the advantage of being mobile, offering targeted high resolution sampling over a potentially large range. These platforms do suffer from power restrictions, with high power consumption required for locomotion, GPS navigation, control and live data transfer. The Wave Glider, is a unique hybrid USV and UUV ([1], [2], [3], [4]) that makes use of a novel wave propulsion mechanism to drive the platform forwards thorough the use of wave action. This reduces onboard power consumption, greatly extending mission duration which makes the Wave Glider an excellent marine research platform ([5], [6], [7]).

Wave glider platforms must operate over extended periods of time in highly dynamic marine environments that are affected by currents, winds and a range of sea states. It is important to understand how the platform performs within this real-world environment as model fidelity limits platform autonomy because realistic interaction models are needed to improve platform control, path planning and navigation.

\*This work was supported by: The South African International Marine Institute, a joint South African Department of Science and Technology and Council for Scientific and Industrial Research Robotics Strategy of South Africa (ROSSA) Grant, and a National Research Fund (NRF) Scarce Skill Scholarship.

<sup>1</sup>Robyn Verrinder and Edward Boje are with the Department of Electrical Engineering, University of Cape Town, South Africa. name.surname@uct.ac.za

In this paper we develop a comprehensive three-dimensional dynamic model of the Liquid Robotics Wave Glider, SV3 ([3]). This model has sufficient fidelity, in terms of the propulsion mechanism, to capture the platform dynamics. The relationship between the float, tether and glider reference frames is described using Denavit-Hartenberg (D-H) parametrization, with Lagrangian modelling used to produce the equations of motion for the system. Physical dimensions and hydrodynamic factors were determined from both a SolidWorks model and through measurements of a Wave Glider SV3 platform. The derived dynamic model is simulated for a given sea state and simple three-dimensional sinusoidal sea states.

## II. BACKGROUND

Modelling of the wave glider platform is developed from the well-established field of ship modelling. Unmanned single bodied vessels that make use of propellers for propulsion include Remotely Operated Vehicles (ROVs) and Autonomous Underwater Vehicles (AUVs), have a depth of research behind them. Buoyancy controlled underwater gliders (UWG) ([8]) have shown promise as an option for underwater ocean research. Dynamic models of all these vessels derive from a single body modelling approach that lacks the degrees of freedom to incorporate coupled surface and underwater components of the Wave Glider. Investigations into the modelling of multi-body platforms have been made, such as by [9], who presented a UWG concept that allows for the transformation between the UWG and a hybrid surface and underwater vessel. The model made use of D-H approach to generate a longitudinal profile for the UWG, but the dynamic principles used in this model cannot be extended to hybrid unmanned surface and underwater vessels that are wave driven. [10] and [11] generated a dynamic model of an earlier version of the platform, the Wave Glider SV2, that represented the system as a single body attached by the tether with two weights on either end, relating to the glider and the float. [12] produced a dynamic model of a multi-body wave-driven surface vessel, but did not consider the hydrodynamic effects on the behaviour of the system. [13] develop a 4 DoF (surge, sway, heave, and yaw) multi-body model of a Wave Glider and test it against sea states predicted using the JONSWAP spectrum.

Regression modelling of the Wave Glider has been investigated to develop kinematic models of the system. [14] made use of linear regression modelling based on sea parameters to generate an estimate of the Wave Glider speed. [15] extended the study to include non-linear regression methods, specifically Gaussian Process Regression with Bootstrap Aggregating based on environmental parameters.[16] extended further by

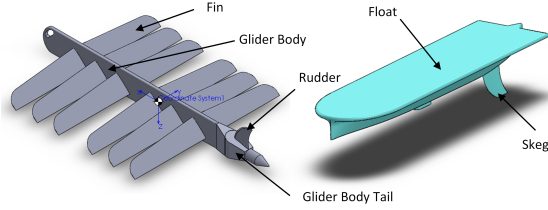


Fig. 1. SolidWorks models of the glider and float subsystems for the SV3 Wave Glider.

incorporating a wave model (WAVEWATCH III) to generate velocity estimates. Regression techniques use averaged or forecast sea parameters rather than the current sea state and are therefore suitable for off-board rather than on-board planning.

A comprehensive three dimensional model of the Wave Glider, including hydrodynamic parameters and attitude dynamics is the focus of this paper. It will be used in future studies to optimise motion control of the platform. The effect of different (sinusoidal) sea states is investigated in simulation to illustrate the utility of our model.

### III. PROPULSION MECHANISM

The Wave Glider platform has three main components: a surface float that provides buoyancy and storage space for the core electronics module (instrumentation payload, solar panels, batteries); an umbilical tether that couples the float and the underwater glider, and allows for control signals and electrical power transmission for actuation of the glider rudder and thruster; and a submersible glider with six hinged hydrofoil fins that pivot near the leading edge and are attached to restorative springs (Fig. 1).

The Wave Glider converts wave energy into forward thrust due to the relative positioning of the float and glider in high and low wave energy zones, respectively. As a wave crest passes under the float, the buoyant structure moves upwards, transferring force through the tether and creating vertical relative motion between the glider and the water. The glider fins are attached to springs in such a way that rotation of the fins is resisted. As the vertical motion of the glider deflects the fins (up or down), an equilibrium angle of attack is reached when the spring force is balanced by the force of the water deflecting the hydrofoil or the maximum angle is reached and the hydrofoil rotation is stopped by mechanical stops. The relative motion of the glider through the water and angle of the hydrofoil generates a hydrodynamic force which has a forward component, thus generating thrust ([1] and [10]). This process occurs as the glider is ascending and descending, due to the range of motion of the fins. This passive propulsion system allows for missions of up to a year before retrieval ([3]).

### IV. DENAVIT-HARTENBERG PARAMETRISATION

A modified D-H ([17] and [18]) system of referencing was chosen to relate the multiple bodies of the system. The D-H parameters for the three dimensional Wave Glider model are given in Table I and the relevant frames shown in Fig.

TABLE I  
D-H PARAMETERS FOR THE THREE DIMENSIONAL MODEL OF THE WAVE GLIDER.

Frame	$a$	$\alpha$	$d$	$\theta$	Joint variable	Frame location
1	0	$-\pi/2$	$y_f$	$-\pi/2$	$y_f$	Float
2	0	$-\pi/2$	$x_f$	$-\pi/2$	$x_f$	Float
3	0	$-\pi/2$	$z_f$	$-\pi/2$	$z_f$	Float
4	0	0	0	$\psi_f$	$\psi_f$	Float
5	0	$-\pi/2$	0	$-\pi/2 + \theta_f$	$\theta_f$	Float
6	0	$-\pi/2$	0	$\phi_f$	$\phi_f$	Float
7	0	0	0	$-\phi_f + \phi_t$	$\phi_t$	Tether
8	0	$\pi/2$	0	$-\theta_f + \theta_t$	$\theta_t$	Tether
9	$l_t$	$-\pi/2$	0	$-\phi_f + \phi_g$	$\phi_g$	Glider
10	0	$\pi/2$	0	$-\theta_f + \pi/2 + \theta_g$	$\theta_g$	Glider
11	0	$\pi/2$	0	$-\psi_f + \psi_g$	$\psi_g$	Glider
12	0	$-\pi/2$	0	$-\theta_g + \theta_a$	$\theta_a$	Hydrofoil

2. The base frame is the inertial NED frame. Frames 1, 2 and 3 are displacements  $y_f$ ,  $x_f$  and  $z_f$  along the joint axes respectively allowing for linear displacement of the float in the inertial frame. Frames 4, 5 and 6 are fixed onto the float body and allow for yawing, pitching and rolling of the float,  $(\psi_f, \theta_f, \phi_f)$  respectively. Frames 7 and 8 are fixed at the connection between the float and tether and allow for rolling and pitching of the tether,  $(\phi_t, \theta_t)$ , respectively. Frames 9, 10 and 11 are fixed on the glider body which is located a distance  $l_t$  along the tether, and these frames allow for rolling, pitching and yawing of the glider,  $(\phi_g, \theta_g, \psi_g)$  respectively. Finally frame 12 allows for pitching of the hydrofoils,  $\theta_a$ , and is fixed onto the first set of hydrofoils. The generalised coordinates  $q = [x_f, y_f, z_f, \phi_f, \theta_f, \psi_f, \phi_t, \theta_t, \phi_g, \theta_g, \psi_g, \theta_a]$  define the 12 degree of freedom system.

### V. LAGRANGIAN MODELLING

Lagrangian modelling was chosen to determine the motion of the system as this eliminates the need to calculate the constraint forces within the system and is easy to apply to multi-body systems. During the modelling process the assumption of a rigid tether was made, which is reasonable as during the operation of the Wave Glider the tether generally remains taut. As the float crests a wave the glider will be lifted by the float and as the float dips into a trough the glider will be pulled down due to gravity. In both cases the glider will be propelled forward, always leading to the tether remaining taut. The range of motion of the hydrofoils was limited by increasing the spring constant of the restorative springs when the hydrofoil angle was greater than  $40^\circ$  or less than  $-20^\circ$  with respect to the glider rather than using a hard non-linear saturation.

The positions,  $p$ , of the centres of mass (C) for the bodies in the system (float, tether, glider, and hydrofoils) take the general form (1) where  $T_0^n$  represents the transform of the bodies' centres of mass from the relevant body D-H frame to the inertial frame. The velocities take the general form (2). For convenience, the total kinetic and potential energy are represented as sums for the bodies in the system in (3) and

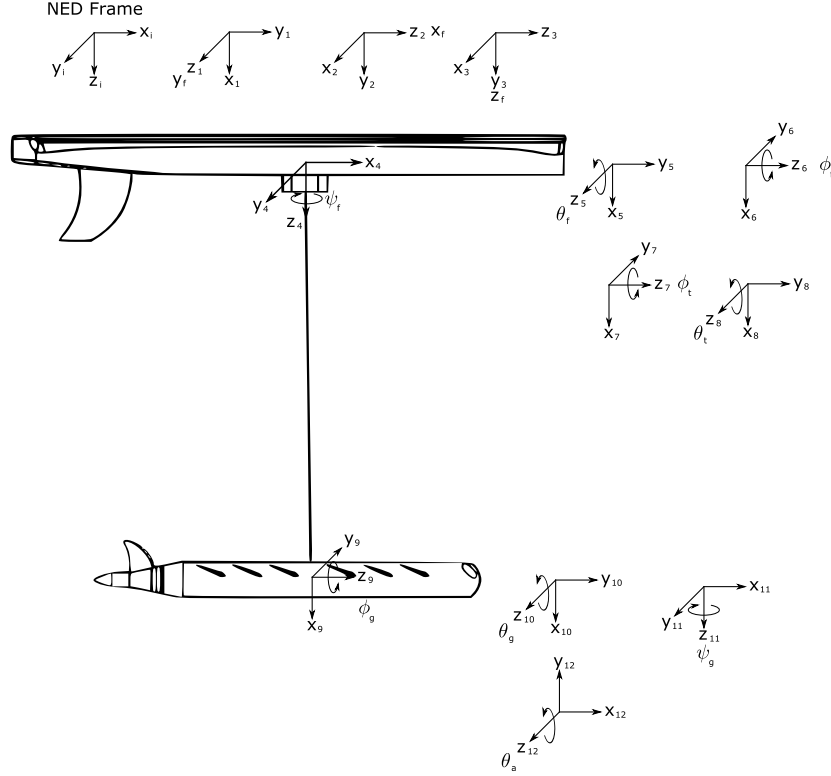


Fig. 2. D-H parametrization of Wave Glider system. The generalised coordinates are shown, where the linear translations of the float are given by  $x_f, y_f$  and  $z_f$ . The angular rotations of the float are  $\phi_f, \theta_f$  and  $\psi_f$ , tether are  $\phi_t$  and  $\theta_t$ , glider are  $\phi_g, \theta_g$  and  $\psi_g$ , and hydrofoils is  $\theta_a$ .

(4) respectively. For a given body,  $m_i$  is the mass of the body,  $v_i$  is the translational velocity of the centre of mass,  $I_i$  is the moment of inertia matrix,  $\omega_i$  is the angular velocity and  $h_i$  is the height of the centre of mass in the inertial plane.

$$p(q) = T_0^n C, \quad (1)$$

$$v = \frac{\partial p}{\partial q} \dot{q}, \quad (2)$$

$$T = \sum_i \left( \frac{1}{2} m_i v_i^T v_i + \frac{1}{2} \omega_i^T I_i \omega_i \right), \quad (3)$$

$$U = \sum_i m_i g h_i. \quad (4)$$

Following the definition of the system's energy the Lagrangian can be constructed,  $L = T - U$ , and the Lagrange equations of motion defined in (5) where  $\tau$  represents the external forces on the system and  $j = 1 \dots n$  where  $n$  is the number of generalised coordinates,

$$\frac{d}{dt} \left( \frac{\partial L}{\partial \dot{q}_j} \right) - \frac{\partial L}{\partial q_j} = \tau_j. \quad (5)$$

We can express these equations in a form comparable to classical ship modelling equations of motion by generating the vector representation, (9), in terms of the rigid-body Mass ( $\mathbf{M}_{RB}$ ), Coriolis and centripetal ( $\mathbf{C}_{RB}$ ), and Restorative vector ( $G$ ) ([19]), where  $\tau$  represents the external forces and torques,

$$\mathbf{M}_{RB} = \frac{d}{dq} \left( \left( \frac{dT}{dq} \right)^T \right), \quad (6)$$

$$[\mathbf{C}_{RB}]_{ij} = c_{ij} = \frac{1}{2} \sum_{k=1}^n \left( \frac{\partial M_{ij}}{\partial q_k} + \frac{\partial M_{ik}}{\partial q_j} + \frac{\partial M_{jk}}{\partial q_i} \right) \dot{q}_i, \quad (7)$$

$$G = \left( \frac{dU}{dq} \right)^T, \quad (8)$$

$$\mathbf{M}_{RB}(q) \ddot{q} + \mathbf{C}_{RB}(q, \dot{q}) \dot{q} + G(q) = \tau. \quad (9)$$

## VI. HYDROSTATIC AND HYDRODYNAMIC FORCES

The glider and float subsystems of the SV3 Wave Glider were modelled in SolidWorks using measured dimensions of an existing platform as manufacturer drawings were not available. The basic shapes were created and approximations made for complex shapes such as the hull of the float. Fig. 1 shows views of the glider and float CAD models.

### A. Buoyancy

The buoyancy was calculated outside of the Lagrangian because of the non-conservative nature of the buoyancy force which is dependent on the volume of water displaced by the system. The buoyancy forces were calculated for each body

separately and then transformed into the inertial frame. The force on the float depends on the displaced volume of the float and its subsequent centre of buoyancy, CB, calculated using a Delauney triangulation approximation. The force on the glider made use of the displaced volume and CB from the SolidWorks model. The buoyancy force provided by the tether was assumed to be negligible.

Making use of the principle of virtual work,  $\delta w$ , expressed in (10) for a force,  $f_i$ , acting at a distance,  $r_i$ , the buoyancy force is treated as a generalised force,  $Q_b$ , with general form given in (11) for the component in the  $j^{\text{th}}$  generalised coordinate,

$$\delta w = \sum_i f_i \cdot \delta r_i = \sum_j Q_j \delta q_j, \quad (10)$$

$$Q_j = \sum_i^n f_i \cdot \frac{\partial r_i}{\partial q_j}. \quad (11)$$

### B. Hydrodynamic Force and Added Mass

It is important to establish reasonable estimates for the hydrodynamic force and added mass characteristics of the glider and float to produce realistic behaviour in the model. SolidWorks Flow Simulation software was utilised to characterise the hydrodynamic forces on the float, glider and hydrofoils separately because of its ease of use and its successful implementation to a reasonable degree of accuracy in other literature ([20]). Analytical methods were used to approximate the added mass values.

The flow simulations conducted on the float were in each of the six body-fixed directions of motion. The linear drag due to sway and the rotational drag components were determined for the glider. For the hydrofoils the linear drag on the glider due to surge and heave for relative angles of the hydrofoils and the glider were determined as well as the rotational drag on the hydrofoil. Each simulation was run at six different fluid velocities and the forces and torques along each body axis, as defined at the centre of gravity (C), were set as convergence goals for the SolidWorks Flow Solver.

Classically, hydrodynamic force factors are arranged in a matrix representing forces imparted due to motion along a particular body axis. The hydrodynamic force from the complete motion vector of the body can then be linearly superimposed ([21]). Since SolidWorks Flow Simulation can provide the forces and torques on a body for a given fluid velocity vector, the data from the flow simulations were used to fit third order polynomial data curves, where the relative velocity of the body and the water could be used directly in the fitted curve equation to find the hydrodynamic force or torque component due to motion along that axis.

The hydrodynamic force associated with the rotational body axes was approximated by emulating a rotating fluid domain. In the case of the float, which will not be fully submerged, the flow simulation was applied as if to a submerged body, but only the forces on expected submerged surfaces of the float were calculated using surface goals in SolidWorks Flow Simulation.

The hydrodynamic force acting on a body in terms of the body-fixed velocities thus took the form of (12) where the notation used denotes, for example, a hydrodynamic force  $X$  in the body-fixed  $x$  direction due to a velocity in the  $z$  direction as  $X_z$ . The hydrodynamic forces were functions of the respective body-fixed velocities in terms of  $q$  and  $\dot{q}$ . The body-fixed linear hydrodynamic forces were transformed into the inertial frame by treating them as generalised forces acting on the relevant body, whereas the rotation hydrodynamic moments could be treated as inertial, such that the hydrodynamic forces in the inertial frame are  $Q_d$ .

$$\mathbf{D}(q, \dot{q}) = \begin{bmatrix} X_x(q, \dot{q}) & X_y(q, \dot{q}) & X_z(q, \dot{q}) & X_\phi(q, \dot{q}) & X_\theta(q, \dot{q}) & X_\psi(q, \dot{q}) \\ Y_x(q, \dot{q}) & Y_y(q, \dot{q}) & Y_z(q, \dot{q}) & Y_\phi(q, \dot{q}) & Y_\theta(q, \dot{q}) & Y_\psi(q, \dot{q}) \\ Z_x(q, \dot{q}) & Z_y(q, \dot{q}) & Z_z(q, \dot{q}) & Z_\phi(q, \dot{q}) & Z_\theta(q, \dot{q}) & Z_\psi(q, \dot{q}) \\ \Phi_x(q, \dot{q}) & \Phi_y(q, \dot{q}) & \Phi_z(q, \dot{q}) & \Phi_\phi(q, \dot{q}) & \Phi_\theta(q, \dot{q}) & \Phi_\psi(q, \dot{q}) \\ \Theta_x(q, \dot{q}) & \Theta_y(q, \dot{q}) & \Theta_z(q, \dot{q}) & \Theta_\phi(q, \dot{q}) & \Theta_\theta(q, \dot{q}) & \Theta_\psi(q, \dot{q}) \\ \Psi_x(q, \dot{q}) & \Psi_y(q, \dot{q}) & \Psi_z(q, \dot{q}) & \Psi_\phi(q, \dot{q}) & \Psi_\theta(q, \dot{q}) & \Psi_\psi(q, \dot{q}) \end{bmatrix} \quad (12)$$

Added mass is a representation of pressure induced forces that are proportional to the acceleration of a body through a fluid. In water, added mass characteristics are not negligible and therefore should be represented in the model. Typically, the added mass is represented in a matrix of the same dimensions as the simulated system. The elements in the matrix are related to the geometry of a body and the properties of the fluid with which it is interacting. The shape of the body may result in an induced acceleration of the fluid in a different direction to the motion of the body, representing the off-diagonal elements of the added mass matrix. However, it is difficult to determine the off diagonal terms in an experimental set-up and without the aid of advanced computational tools. For this initial study the added mass characteristics were approximated using analytical data ([22, 23]). Due to the uncertainty in applying analytical methods to a complex shape, it was assumed that the body was symmetrical in three planes and that any off-diagonal added mass elements would be negligible compared to the diagonal elements. In addition, it was assumed that the change in added mass properties due to movement of the fins on the glider and the position of the float in the water would have negligible influence at this stage. The body-fixed added mass terms were transformed into the inertial frame making use of a kinetic energy representation, (3), to determine the added mass and added Coriolis and centripetal matrices making use of the same methods used to determine the rigid-body matrices.

When considering the effect that these hydrostatic and hydrodynamic forces have the final dynamic model takes the form of (13) with  $\mathbf{M}_A$  and  $\mathbf{C}_A$  representing the added mass terms,  $Q_d$  representing the hydrodynamic force, and  $Q_b$  representing the hydrostatic forces.

$$(\mathbf{M}_{RB}(q) + \mathbf{M}_A(q))\ddot{q} + (\mathbf{C}_{RB}(q, \dot{q}) + \mathbf{C}_A(q, \dot{q}))\dot{q} + G(q) + Q_b(q) + Q_d(q, \dot{q}) = \tau. \quad (13)$$

## VII. SIMULATED RESULTS

The model parameters used in the simulations are shown in Table II. The system was simulated making use of a sinusoidal sea state with a frequency of 0.1 Hz and a peak-to-peak

TABLE II  
MODEL PARAMETERS FOR SIMULATED RESULTS.

Parameters	Value
$m_f$	50 kg
$m_t$	10 kg
$m_g$	150 kg
$C_f$	[0, 0, 0] m
$C_t$	[0, 0, 0] m
$C_g$	[0, 0, 0] m
$CB_g$	[-0.09, 0, 0.08] m
$I_f$	diag(2.95, 38.98, 41.49) kg·m <sup>2</sup>
$I_t$	diag(53.33, 53.33) kg·m <sup>2</sup>
$I_g$	diag(25.76, 57.26, 81.92) kg·m <sup>2</sup>
$l_t$	4 m
$M_{A_f}$	diag(-66.18,-157.02,-334.706,-1.87,-49.47,46.77)
$M_{A_g}$	diag(-268.10,-73.78,-207.28,-105.38,-65.31,-106.09)

amplitude of 1.5 m to represent typical swell waves. The sea state used in the simulations took the form of a wave field with specified boundaries.

#### A. Model Validity

Several tests were conducted to determine if the hybrid USV-UUV model acted as expected. Firstly the system's vertical response to the given sea state is shown in Fig. 3. For the sinusoidal sea state with a peak-to-peak amplitude of 1.5 m it can be seen that the height of the float,  $z_f$ , follows the wave height closely. There are small irregularities as the float crests the waves, likely due to the variable added mass of the glider dependent on the glider orientation. In Fig. 4 the pitch angle of the float,  $\theta_f$ , follows that of the relevant gradient of the sea state with some oscillations due to the tether. Some lag exists in the response which can be attributed to the inertia of the float as well as the buoyancy being calculated using a tangential wave surface positioned at the centre of the float body.

Fig. 5 shows the relationship between the glider height and the glider  $x$ -velocity. It can be seen that the glider velocity increases as the glider is pulled out of the water and decreases as the glider moves into the water, which is due to the characterisation of the hydrofoil. When considering the effect this has on the float, it has an average velocity of  $0.60 \text{ m}\cdot\text{s}^{-1}$ , which falls within the expected values for the Wave Glider in typical sea conditions.

#### B. Response to directional sea state

In order to determine if the path taken through a specific sea state could be utilised for path planning, the model was tested for wave fronts approaching the vessel at different angles. Tests were conducted for sea states with a peak-to-peak amplitude of 1.5 m with a frequency of 0.1 Hz. Fig. 6 shows the average speed of the float for this sea state approaching the vessel from different angles. It can be seen that the relative

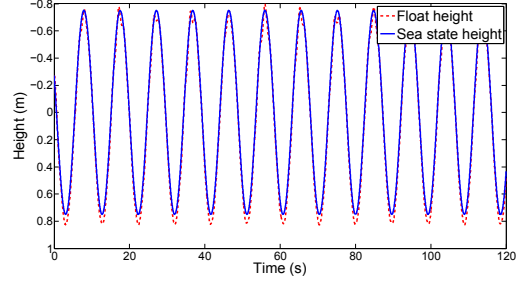


Fig. 3. The system vertical response to traversing a given sea state. The height of the centre of the float,  $z_f$ , follows the height of the sea state closely.

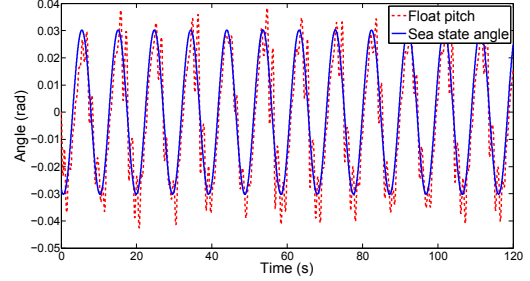


Fig. 4. The pitch angle of the float,  $\theta_f$ , follows the relevant gradient of the sea state at the position of the float,  $w_a$ , with some lag. Oscillations in the pitch of the float are likely due to the buoyancy moment and tether forces.

heading of the Wave Glider into the wave has a small role in the platform's average speed as there is approximately a 25% increase in the average speed of the platform when comparing incident wave approaching from  $0^\circ$  and from  $180^\circ$ .

## VIII. CONCLUSIONS AND FUTURE WORK

A detailed three dimensional Lagrangian dynamic model including buoyancy, added mass and hydrodynamic damping using the D-H referencing system has been presented. The model characterises the hydrofoil motion to determine the propulsion based on the sea state. The simulation results show that the model is plausible for a given sea state, and gives expected velocities when compared to previous mission data

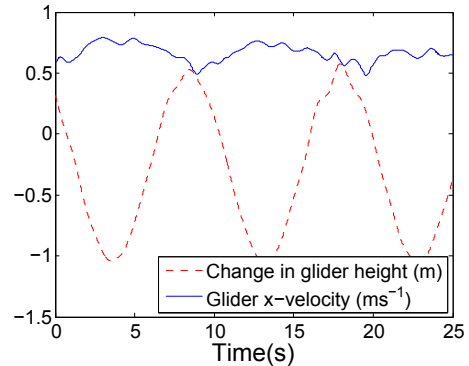


Fig. 5. Glider height and velocity. The glider velocity increases as the glider moves out of the water, and decreases but remains positive as the glider moves into the water.

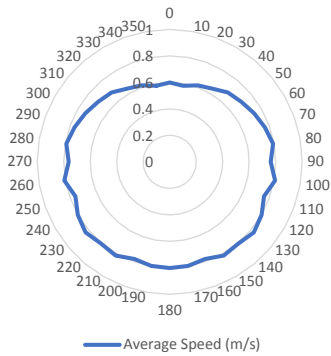


Fig. 6. Polar plot showing float average speed for relative sea state angles. An increase in the average speed can be seen as the angle between the sea state and the direction of motion of the Wave Glider model increases to 90°, after which the average velocity remains relatively constant.

([1] and [6]). The results show that for this marine vessel the heading relative to the wave-front can affect the platform's performance. An understanding of the interaction between the Wave Glider and the sea state is required to improve path planning, navigation and power consumption. Future work will include consideration of currents and wind induced forces.

#### REFERENCES

[1] R. Hine and P. A. McGillivray, "Wave powered autonomous surface vessels as components of ocean observing systems," in *Pacific Congress on Marine Science and Technology (PACON 2007)*, Honolulu, HI, 2007.

[2] J. E. Manley and S. Willcox, "The Wave Glider: A persistent platform for ocean science," in *OCEANS 2010 IEEE-Sydney*, Sydney, 2010, pp. 1–5.

[3] 2016, accessed: 2016-08-01. [Online]. Available: <http://www.liquid-robotics.com>

[4] J. E. Manley, R. Carlon, and G. Hine, "Ten years of wave glider operations: A persistent effort," in *OCEANS 2017 - Anchorage*, 2017, pp. 1–5.

[5] T. Daniel, J. E. Manley, and N. Trenaman, "The Wave Glider: Enabling a new approach to persistent ocean observation and research," *Ocean Dynamics*, vol. 61, no. 10, pp. 1509–1520, 2011.

[6] S. Frolov, J. G. Bellingham, W. Anderson, and G. Hine, "Wave Glider - A platform for persistent monitoring of algal blooms," in *OCEANS'11 MTS/IEEE KONA*, Waikoloa, HI, 2011, pp. 1–5.

[7] T. W. Rochholz, "Wave-powered unmanned surface vehicle as a station-keeping gateway node for undersea distributed networks," MSc. Thesis in Applied Physics, Naval Postgraduate School, 2012. [Online]. Available: <https://calhoun.nps.edu/handle/10945/17448>

[8] N. E. Leonard and J. G. Graver, "Model-based feedback control of autonomous underwater gliders," *IEEE Journal of Oceanic Engineering*, vol. 26(4), pp. 633–645, 2001.

[9] A. Caiti, V. Calabró, S. Grammatico, A. Munafó, and M. Stifani, "Lagrangian modelling of an underwater wave glider," *Oceans 2011*, pp. 6–9, 2011.

[10] N. Kraus and B. Bingham, "Estimation of wave glider dynamics for precise positioning," in *OCEANS 2011*. IEEE, 2011, pp. 1–9.

[11] N. D. Kraus, "Wave glider dynamic modelling, parameter identification and simulation," Master's thesis, University of Hawai'i, 2012.

[12] B. Tian, J. Yu, and A. Zhang, "Lagrangian dynamic modeling of wave-driven unmanned surface vehicle in three dimensions based on the dh approach," *IEEE International Conference on Cyber Technology in Automation, Control and Intelligent Systems*, pp. 1253–1258, 2015.

[13] P. Wang, X. Tian, W. Lu, Z. Hu, and Y. Luo, "Dynamic modeling and simulations of the wave glider," *Applied Mathematical Modelling*, vol. 66, pp. 77–96, 2019.

[14] R. N. Smith, J. Das, G. Hine, W. Anderson, and G. S. Sukhatme, "Predicting wave glider speed from environmental measurements," in *OCEANS 2011*. IEEE, 2011.

[15] P. Ngo, W. Al-Sabban, J. Thomas, W. Anderson, J. Das, and R. N. Smith, "An analysis of regression models for predicting the speed of a wave glider autonomous surface vehicle," in *Proceedings of Australasian Conference on Robotics and Automation*. Australian, 2013, pp. 1–9.

[16] P. Ngo, J. Das, J. Ogle, J. Thomas, W. Anderson, and R. N. Smith, "Predicting the speed of a wave glider autonomous surface vehicle from wave model data," *2014 IEEE/RSJ International Conference on Intelligent Robots and Systems*, pp. 2250–2256, 2014.

[17] J. Denavit and R. S. Hartenberg, "A kinematic notation for lower-pair mechanisms based on matrices," *Journal of Applied Mechanics, Transactions ASME*, vol. 22, pp. 215–221, 1955.

[18] B. Siciliano and O. Khatib, *Springer Handbook of Robotics*. Springer, 2008, vol. 53.

[19] R. M. Murray, Z. Li, S. S. Sastry, and S. Sastry, S, *A mathematical introduction to robotic manipulation*. CRC press, 1994.

[20] O. A. Eidsvik, "Identification of hydrodynamic parameters for remotely operated vehicles," Master's thesis, NTNU, 2015.

[21] O. Faltinsen, *Sea loads on ships and offshore structures*. Cambridge university press, 1993, vol. 1.

[22] DNV, "Recommended practice dnv-rp-h103, modelling and analysis of marine operations," Det Norske Veritas, Tech. Rep., 2014.

[23] C. E. Brennen, "A review of added mass and fluid inertial forces." Naval Civil Eng. Laboratory, Tech. Rep., 1982.